agriculture

MDPI

Article

Soil Vapor Extraction Reduces Gas-Phase MITC and Subsequent Phytotoxicity After Dazomet Fumigation

Yi Zhang [1], Xiujun Tang [2], Yutong Ji [3], Yuan Li [3], Wensheng Fang [3], Dongdong Yan [3], Aocheng Cao [3] and Qiuxia Wang [3,*]

[1] Agro-Environmental Protection Institute, Ministry of Agriculture and Rural Affairs, Tianjin 300191, China; zhangyi10@caas.cn
[2] School of Plant Protection, Anhui Agricultural University, Hefei 230036, China; tangxj@ahau.edu.cn
[3] State Key Laboratory for Biology of Plant Disease and Insect Pests, Institute of Plant Protection, Chinese Academy of Agricultural Sciences, Beijing 100193, China; jiyutong59@163.com (Y.J.); liyuancaas@126.com (Y.L.); fws0128@163.com (W.F.); 13260176634@163.com (D.Y.); caoac@vip.sina.com (A.C.)
* Correspondence: qxwang@ippcaas.cn

Abstract

Dazomet (DZ) is widely used for soil fumigation, but its active product methyl isothiocyanate (MITC) may persist after treatment and cause phytotoxicity to subsequent crops. This study evaluated a portable activated-carbon-coupled soil vapor extraction (SVE) system for post-fumigation management of residual MITC. An L9 (3^3) orthogonal experiment was used to optimize MITC recovery from activated carbon, and field experiments were conducted at two agricultural sites in Beijing. At each site, three SVE plots and three concurrently fumigated no-SVE control plots were established. Ethyl acetate extraction at an activated-carbon-to-solvent ratio of 1:1 with 120 min oscillation provided recoveries of 84.5–98.6%. During SVE operation, changes in gas-phase and soil-phase MITC concentrations were observed within the treated plots, and MITC was recovered from the activated-carbon cartridges. After 7 days of laboratory aeration, SVE-treated soils supported complete cucumber germination and improved seedling growth relative to fumigated no-SVE controls, indicating reduced residual phytotoxicity under the tested bioassay conditions. Soil-phase MITC increased during the same interval, suggesting redistribution of MITC between phases and possibly reflecting continued DZ transformation.

Keywords: dazomet; methyl isothiocyanate; soil vapor extraction; aeration; phytotoxicity

1. Introduction

Soil fumigants are widely used for the management of soil-borne pathogens, nematodes, and weeds in intensive agricultural systems. Among them, dazomet (DZ) is a granular soil fumigant that can be easily applied by broadcasting and soil incorporation. After contact with soil moisture, DZ rapidly decomposes to generate methyl isothiocyanate (MITC), the primary active compound responsible for its pesticidal activity [1–6]. MITC exhibits strong biocidal activity by reacting with nucleophilic groups in proteins and enzymes of target organisms [7–9]. However, the same high biological activity and volatility that make MITC effective as a fumigant may also result in prolonged persistence after application, causing phytotoxicity to subsequent crops if residues are not sufficiently dissipated. Post-fumigation aeration is therefore an essential step before crop establishment. Conventional management practices mainly rely on natural volatilization and degradation processes, sometimes combined with irrigation or extended waiting periods, to reduce

Check for updates

Received: 3 September 2026
Revised: 20 October 2026
Accepted: 22 October 2026
Published: 26 October 2026

Copyright: © 2026 by the authors. Licensee MDPI, Basel, Switzerland. This article is an open access article distributed under the terms and conditions of the Creative Commons Attribution (CC BY) license.

residual fumigant concentrations [10–12]. However, prolonged aeration can delay crop production, particularly in intensive cropping systems with short intervals between successive crops. Moreover, uncontrolled volatilization of residual MITC may result in emissions to the surrounding environment and potential exposure of non-target organisms [13–15]. Therefore, developing an effective approach that can accelerate residual fumigant removal while controlling extracted emissions is important for improving the efficiency and safety of soil fumigation practices.

SVE is currently an important method for large-scale removal of volatile organic compounds (VOCs) from soil [16,17]. The principle of SVE is to use vacuum technology to drive soil-directed extraction and flow, converting various pollutants in the soil into gas for removal [18,19]. A typical vapor extraction system includes extraction wells, vacuum pumps, gas-water separation devices, gas collection pipelines, gas purification equipment, and auxiliary equipment [20,21]. However, due to the limitations of soil fumigation application scenarios, installing a vapor extraction system after removing the plastic film over large areas is not practical. Therefore, modifications to the traditional vapor extraction system are necessary to align it with the use of soil fumigants. To the best of our knowledge, the application of SVE technology for post-fumigation management of MITC residues and phytotoxicity has rarely been investigated. Thus, in order to explore techniques for the rapid removal of dazomet residues and phytotoxicity after its use in the field, we employed a high-pressure fan as the extraction device, with activated carbon tubes placed at its outlet to adsorb the extracted fumigant gases. We conducted experiments in Shunyi and Fangshan districts in Beijing to investigate the removal of MITC residues from soil and the reduction in phytotoxicity after dazomet fumigation.

2. Materials and Methods

2.1. Chemicals, Films, and Seeds and Field Site Characterization

Dazomet (98%) was obtained from Nantong Shizhuang Chemical Co., Ltd. (Nantong, China). Ethyl acetate (HPLC grade) and anhydrous sodium sulfate were purchased from Sinopharm Chemical Reagent Co., Ltd. (Shanghai, China); 0.22 μm organic filter membranes were purchased from Tianjin Jinteng Laboratory Equipment Co., Ltd. (Tianjin, China); polyethylene (PE) film (0.04 mm) was obtained from Shandong Shouguang Longxing Agricultural Film Co., Ltd. (Shouguang, China); and 'Zhongnong No. 6' cucumber seeds were purchased from Zhongshu Seed Industry Technology Co., Ltd. (Beijing, China).

Field experiments were conducted at two agricultural sites in Beijing, China, including Hongke Farm in Fangshan District (39°62′96.23″ N, 115°97′92.15″ E) and Shiwaiyuan Farm in Shunyi District (40°02′99.06″ N, 116°77′30.58″ E), Beijing. The soils at both sites were classified as sandy loam soils. Before fumigation, soil samples were collected for physicochemical characterization. The soils contained different levels of available nutrients and chemical properties. In Shunyi and Fangshan soils, ammonium nitrogen concentrations were 21.11 and 15.96 mg kg^{-1}, nitrate nitrogen concentrations were 307.73 and 105.85 mg kg^{-1}, available phosphorus concentrations were 345.46 and 716.24 mg kg^{-1}, and rapidly available potassium concentrations were 1900.05 and 2256.50 mg kg^{-1}, respectively. Organic matter contents were 35.83 and 37.94 g kg^{-1}, with pH values of 7.18 and 7.25 and electrical conductivities of 2.17 and 0.97 mS cm^{-1}, respectively.

The initial gravimetric soil water content was approximately 12% at both experimental sites. At the time of SVE operation, the gravimetric soil water contents were approximately 12% in Fangshan and 15% in Shunyi. Based on an assumed bulk density of 1.2 g cm^{-3}, the corresponding volumetric water contents were estimated to be 14.4% and 18.0%, respectively. Assuming a particle density of 2.65 g cm^{-3}, the estimated total soil porosity was 54.7% at both sites, corresponding to estimated air-filled porosities of 40.3% in Fang-

shan and 36.7% in Shunyi. These estimated parameters provide basic information on soil physical conditions relevant to gas transport during SVE operation.

2.2. SVE Device

The soil vapor extraction device developed in this study comprised a high-pressure fan, polyethylene tubing, and an activated-carbon tube. The fan (rated power, 180 W; speed, 2800 r min^{-1}; flow rate, 405 m^3 h^{-1}) was purchased from Zhejiang Yinniu Electromechanical Co., Ltd. (Taizhou, China). The polyethylene tubing (10 cm inner diameter; 3 mm wall thickness) was purchased from Shandong Qizheng Engineering Plastics Co., Ltd. (Weifang, China). Cylindrical activated carbon (approximately 4 mm diameter; iodine value, 500 mg g^{-1}) was obtained from Shijiazhuang Hongsen Activated Carbon Co., Ltd. (Shijiazhuang, China). The adsorption tube was assembled in the laboratory by sealing both ends of a 25 cm polyethylene tube with 80-mesh iron wire and filling it with 200 g of activated carbon.

The SVE system is shown in Figure 1. The inlet of the high-pressure fan was connected to a 3 m polyethylene pipe. At 1.65, 1.95, 2.25, 2.55, and 2.85 m from the intake, three 4 cm diameter holes were positioned at 120° intervals, providing 15 uniformly distributed inlet holes. The fan outlet was connected sequentially to a 0.40 m polyethylene pipe and the 0.25 m activated-carbon tube.

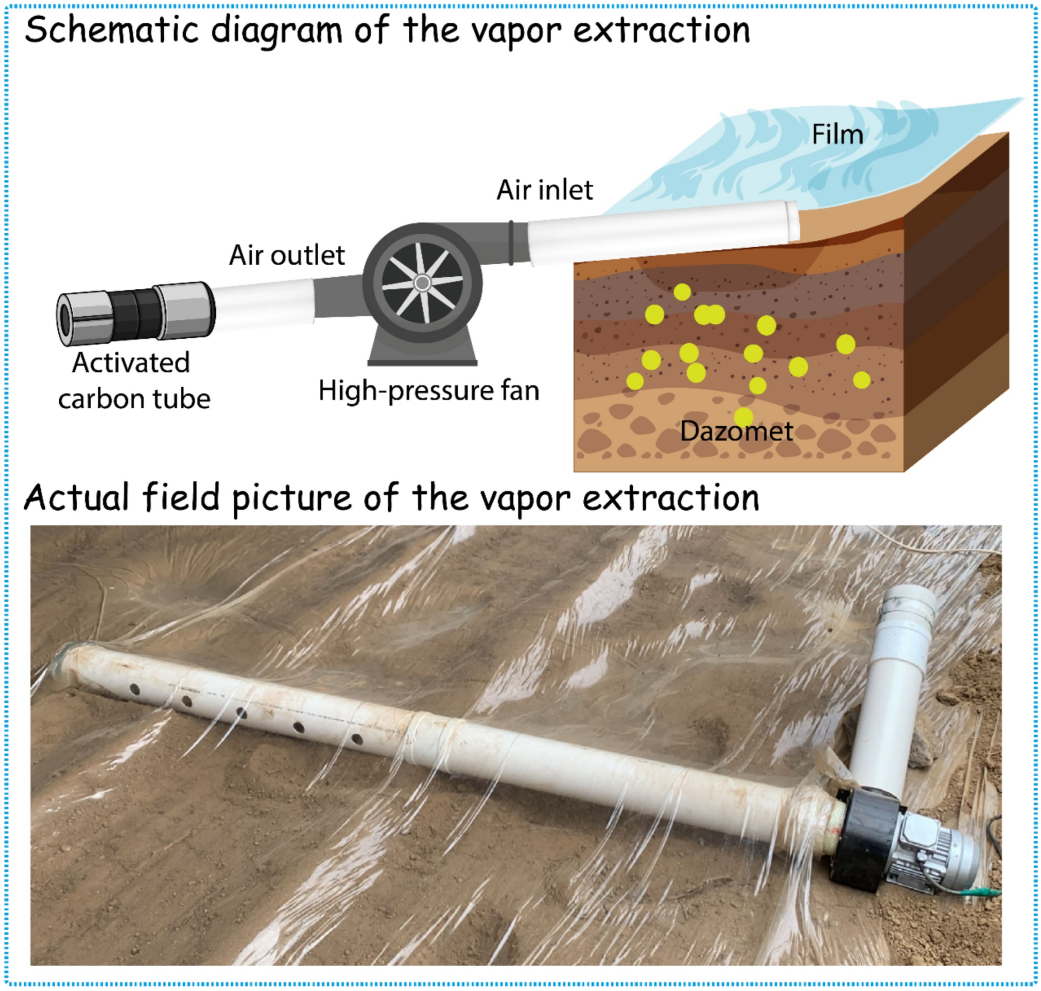

Figure 1. Soil vapor extraction device: schematic configuration and field setup.

2.3. Field Fumigation

Dazomet fumigation was conducted on 14 and 17 July 2022 at Hongke Farm in Fangshan District and Shiwaiyuan Farm in Shunyi District, Beijing, China, respectively. At each site, six independent fumigated field plots were established, including three plots subjected to soil vapor extraction (SVE) and three concurrently fumigated plots without SVE, which served as the fumigated no-SVE controls. No formal blocking design was applied. Each plot at Fangshan measured 42 m^2 (6 × 7 m), whereas each plot at Shunyi measured 60 m^2 (6 × 10 m). A buffer area of 6 × 4 m was maintained between adjacent plots to minimize potential cross-plot interference associated with fumigant movement and SVE-induced gas flow.

Dazomet was applied uniformly to all six fumigated plots at a rate of 50 g m^{-2}. The fumigant was manually broadcast over the soil surface and incorporated into the upper 0–15 cm soil layer using a rotary tiller. Subsequently, the soil was covered with polyethylene (PE) film, and the film edges were compacted to ensure sealing. Following 20 days of film-covered fumigation, SVE was performed independently in the three designated SVE plots at each site, whereas the remaining three fumigated plots did not undergo SVE.

The field plot was considered the independent experimental unit, with three replicates per treatment at each site (n = 3). Sampling locations within each plot were treated as spatial subsamples rather than independent experimental replicates. The detailed sampling procedures are described in Section 2.4.

2.4. SVE Operation and Sampling

After 20 days of film-covered fumigation, the SVE device was installed in the designated plots. The intake pipe was inserted beneath the PE film at the midpoint of the 6 m side of each plot and extended toward the plot center. The outlet of the extraction pipe was sequentially connected to polyethylene tubing and an activated-carbon adsorption tube, and the extraction fan was operated continuously. The activated-carbon tube was replaced every 40 min, resulting in four adsorption samples per plot. Each used tube was immediately sealed, labeled, and stored at −80 °C until MITC analysis. After collection, the spent activated carbon from each cartridge was homogenized, and a representative 5-g subsample was taken for MITC analysis. The subsample was extracted with ethyl acetate using the optimized activated-carbon-to-solvent mass ratio of 1:1 and an extraction time of 120 min. MITC concentrations were determined by GC–MS and expressed as μg g^{-1} of activated carbon. The total amount of MITC retained in each cartridge was estimated by scaling the concentration determined in the subsample to the total activated-carbon mass of 200 g.

For spatial characterization of soil gas and soil-phase MITC, twelve predefined sampling zones were established within each plot according to their relative positions to the extraction pipe. Soil gas samples were collected by withdrawing 20 mL of gas from beneath the PE film using a gas-tight syringe and immediately transferring the sample into a 20 mL headspace vial sealed with an aluminum cap containing a silicone septum. Subsequently, the PE film was carefully slit, and approximately 8 g of soil was collected from the upper 0–15 cm soil layer and transferred into a clean headspace vial. The film opening was immediately resealed with adhesive tape after sampling. Gas-phase and soil-phase MITC concentrations were measured before and after SVE operation within the three designated SVE plots at each site. Corresponding MITC concentration measurements were not obtained from the concurrently fumigated no-SVE control plots. Therefore, the MITC concentration dataset was used to characterize temporal changes within the SVE-treated plots rather than to quantify treatment effects relative to concurrent controls.

To characterize the spatial attenuation of MITC during SVE, distance-based sampling positions were established relative to the distal end of the extraction pipe, which was defined as the reference point (0 m). Five distance classes were selected: −0.5, 0, +0.5, +1.0, and +1.5 m. The −0.5 m position represented a location 0.5 m toward the interior of the extraction pipe from its distal end, whereas the positive distances represented positions extending outward from the pipe end. Four sampling locations were selected within each distance class for both soil gas and soil-phase measurements.

Before and after SVE sampling was conducted using paired spatial locations. Because soil collection was destructive, samples before and after SVE were not collected from exactly the same soil core. Instead, after completion of SVE, samples were collected from adjacent matched locations approximately 10–20 cm away from the original sampling positions within the same predefined sampling zones. These paired locations were matched according to their distance from the extraction pipe and spatial sampling zone to minimize spatial variability while avoiding disturbance caused by previous sampling. All gas and soil samples were immediately transferred to a −80 °C freezer until further analysis.

2.5. Phytotoxicity Testing

The cucumber bioassay was conducted using soils collected from the Fangshan and Shunyi field sites to evaluate the residual phytotoxicity after DZ fumigation and SVE treatment. Four soil groups were evaluated: (1) before-SVE soil, collected from the three designated SVE plots immediately before initiation of the SVE operation; (2) after-SVE soil, collected from the same SVE plots immediately after completion of SVE; (3) fumigated no-SVE control soil, collected from the three concurrently DZ-fumigated plots that received no SVE and sampled at the same time point as the after-SVE treatment; and (4) unfumigated control soil (CK), collected from untreated plots without DZ application, which was used only to establish the baseline germination and seedling growth performance of cucumber.

Each soil group was evaluated after two aeration periods (0 and 7 days). For the 0-day treatment, the cucumber bioassay was initiated immediately after soil collection. For the 7-day treatment, collected soils were placed in open containers and maintained at room temperature for 7 days to allow natural aeration before bioassay. The same aeration procedure was applied to all soil groups. The fumigated no-SVE control plots experienced the same post-fumigation time interval as the SVE-treated plots but did not undergo active vapor extraction. Soil samples from these control plots were used for the cucumber bioassay to evaluate differences in residual phytotoxicity between SVE-treated and untreated fumigated soils. However, MITC concentrations were not determined in the no-SVE control plots.

For SVE and fumigated no-SVE plots, soil samples were collected according to the spatial sampling scheme described in Section 2.4. Within each field plot, approximately 300 g of soil was collected separately from each of the 12 predefined sampling locations, placed in sealed bags, and transported to the laboratory. Samples from different sampling locations were not pooled. Each soil sample was transferred into an individual plastic pot, resulting in 12 pots per field plot. The three independent field plots were considered the experimental replicates (n = 3), whereas the 12 pots within each plot were treated as spatial subsamples rather than independent field replicates.

For each pot, ten cucumber seeds pre-soaked in warm water for approximately 2 h were sown on the soil surface and covered with approximately 1 cm of soil. The pots were watered and incubated in darkness for 3–5 days. Germination rate, root length, and shoot length were subsequently recorded. Phytotoxicity was considered absent when cucumber germination exceeded 80%, was comparable with the unfumigated control,

and no significant inhibition of seedling growth was observed according to previous studies [2,22].

2.6. Extraction and Detection of MITC

Ethyl acetate was selected to extract MITC adsorbed by the activated-carbon tubes. A three-factor, three-level orthogonal experiment based on an L9 (3^3) array was used to optimize the extraction procedure (Table 1).

Table 1. Orthogonal-design factors and levels used to optimize MITC extraction from activated carbon.

Factor	Level		
	1	2	3
Extraction method (A)	Oscillatory extraction	Water bath at 70 °C	Ultrasonic extraction
Extraction time (B)	30 min	60 min	120 min
Activated carbon:solvent (m:m) (C)	3:2	1:1	2:3

Weigh exactly 0.0250 g of MITC standard using a balance with an accuracy of 0.0001 g, dissolve it in ethyl acetate, and dilute it to 25 mL in a volumetric flask to prepare a standard solution with a concentration of 1000 μg mL^{-1}. Using a micropipette, accurately transfer 1, 2, 5, 10, 15, 20, 30, and 40 μL of the MITC standard solution into 20 mL headspace vials and immediately seal with aluminum caps containing silicone septa. The samples are then analyzed by the Agilent 7697A Headspace Sampler, the Agilent 8890 Gas Chromatograph coupled with the 5977B Mass Spectrometer (GC–MS), and an Rtx-5 MS chromatographic column (30 m × 0.25 mm × 0.25 mm), all provided by Agilent Technologies, Santa Clara, CA, USA. These aliquots corresponded to absolute MITC amounts of 1, 2, 5, 10, 15, 20, 30, and 40 μg per vial, respectively. A headspace calibration curve was established by plotting the MITC peak area against the absolute amount of MITC introduced into each vial (μg/vial). This calibration was used for MITC determination by headspace GC–MS.

Separately, a solvent-based calibration curve was established for MITC quantification in ethyl acetate extracts. A series of MITC working standard solutions ranging from 0.005 to 10 mg L^{-1} was prepared by dilution of the stock standard solution with ethyl acetate. The calibration curve was constructed by plotting the MITC peak area against the corresponding solution concentration (mg L^{-1}), using 1/x-weighted linear regression. Next, weigh 5 g of unused activated carbon and place it in the bottom of a clean 20 mL headspace vial. Using a micropipette, accurately transfer 2 μL of the MITC standard solution onto the side wall of the same vial and immediately seal it with an aluminum cap. Carefully transfer the vial to a 45 °C incubator and allow it to incubate for 20 min, enabling the MITC to fully volatilize into the gas phase and be adsorbed by the activated carbon. Then, add varying volumes of ethyl acetate as shown in Table 1, immediately seal the vial with the aluminum cap, and perform extraction using different methods and times. Afterward, analyze the samples using GC–MS and quantify them using the external standard method. The extraction recovery of MITC from fortified activated carbon was calculated using the following equation:

$$REC = \frac{C_{spiked} - C_{blank}}{C_{added}} \times 100\%$$

where *REC* represents the extraction recovery (%); *Cspiked* is the measured MITC concentration in the fortified activated-carbon sample (μg g^{-1}); *Cblank* is the measured MITC concentration in the corresponding unfortified activated-carbon blank (μg g^{-1}); and *Cadded* is the nominal concentration of MITC added during fortification (μg g^{-1}).

Method performance was evaluated using recovery and precision criteria adapted from SANCO/12495/2011 at four spiking levels (0.01, 0.1, 1, and 5 mg kg^{-1}), with five replicates per level. Within-day relative standard deviation (RSDN) was calculated from five replicate recoveries obtained on one day, and between-day relative standard deviation (RSDB) was calculated from measurements obtained on three separate days.

The RSD_N calculation was:

$$RSD_N = \frac{S}{X} \times 100\%$$

For the within-day calculation, S is the standard deviation of five replicate recoveries and X is their mean recovery.

The RSD_B calculation was:

$$RSD_B = \frac{S_B}{X_B} \times 100\%$$

For the between-day calculation, S is the standard deviation of the daily mean recoveries and X is the mean of the three daily means.

Each activated-carbon cartridge contained 200 g of activated carbon and was replaced at 40-min intervals during the 160-min SVE operation. For the analysis of field-exposed cartridges, the activated carbon from each cartridge was thoroughly homogenized, and a representative 5-g subsample was collected for MITC determination using the optimized extraction procedure. The MITC concentration in the activated carbon was calculated from the concentration measured in the extract, the extraction solvent volume, and the subsample mass. The blank-corrected MITC content (q_i, μg g^{-1}) was calculated as follows:

$$q_i = \frac{[(C_I - C_{\beta,i})] \times V_i \times D_i}{m_i}$$

where C_i and $C_{\beta,i}$ are the MITC concentrations in the sample extract and corresponding procedural blank (μg mL^{-1}), respectively; V_i is the extraction solvent volume (mL); D_i is the dilution factor; and m_i is the mass of activated carbon analyzed (g).

The estimated MITC mass retained in each cartridge (Q_i, μg) was obtained by multiplying the MITC content by the total activated-carbon mass (M = 200 g):

$$Q_i = q_i \times M$$

No recovery correction was applied to the field samples, as the validated extraction method demonstrated acceptable recoveries (84.5–98.6%) and precision (RSD, 1.8–8.0%). Therefore, the reported MITC amounts represent blank-corrected but recovery-uncorrected estimates.

The cumulative MITC mass recovered from the four consecutive cartridges was calculated as the sum of the individual cartridge amounts, and the average MITC recovery rate for each sampling interval was obtained by dividing the corresponding cartridge amount by the sampling duration of 40 min. Although analytical precision was evaluated during method validation, uncertainty associated with subsampling the homogenized activated carbon was not independently quantified. Therefore, complete uncertainty propagation for the cartridge-level MITC estimates was not possible.

The soil residue extraction method for MITC follows the procedure described [12]. After removing the headspace vial from the −80 °C freezer, wipe off any surface moisture and immediately weigh the vial. The weight of the vial and cap is subtracted to record the precise weight of the soil inside the vial. Next, quickly open the vial, add 8 mL of ethyl

acetate and 5.6 g of anhydrous sodium sulfate, and immediately reseal the vial. Place the vial on a shaker and shake at 2500 rpm for 60 min. Afterward, allow it to stand at room temperature for 30 min. The vial is then opened, and 2 mL of the supernatant is drawn using a syringe. The supernatant is filtered through a 0.22 μm organic filter membrane and transferred to a 2 mL clear injection vial for GC–MS analysis.

The GC–MS detection conditions are as follows: Helium is used as the carrier gas with a flow rate of 1.5 mL min^{-1}. The injection port temperature is set at 250 °C, and the oven temperature is held at 50 °C for 5 min. The ion source temperature is 230 °C, and the transfer line temperature is 180 °C. The analysis is conducted in Selective Ion Monitoring (SIM) mode, monitoring fragment ions with m/z values of 45 and 73. Under these conditions, the retention time for MITC is 3.4 min, with a Limit of Quantification (LOQ) of 10 μg kg^{-1}. For MITC gas samples, headspace injection is used, with the heating furnace, quantitative ring, and transfer line temperatures set at 100 °C, 115 °C, and 118 °C, respectively. The equilibration time is 2.2 min, and the LOQ for MITC gas samples is 0.001 μg mL^{-1}. Both MITC gas and soil samples are quantified using the external standard method.

2.7. Statistical Analysis

Statistical analyses were performed using IBM SPSS Statistics version 19.0. The field plot was considered the independent experimental unit, whereas measurements from different sampling locations within each plot were treated as spatial subsamples. For soil-phase MITC concentrations, measurements from the same three SVE-treated plots before and after SVE operation were compared using paired-samples *t*-tests to account for the repeated-measurement structure ($n = 3$ independent plots per site). Measurements from spatial sampling locations were summarized at the plot level before statistical analysis. Fangshan and Shunyi were analyzed separately, and the paired mean differences and corresponding 95% confidence intervals were calculated. Statistical significance was evaluated at $p < 0.05$. Given the limited number of independent field replicates, the statistical results were interpreted cautiously. Measurements below the LOQ were reported as <LOQ rather than assigned numerical values. No substitution with zero, LOQ/2, or other estimated values was applied. These measurements were excluded from quantitative statistical comparisons requiring numerical concentration values. Consequently, gas-phase MITC data containing values below the LOQ were summarized descriptively without inferential significance testing.

For cucumber bioassay data, field plots were considered biological replicates, while measurements from individual pots within each plot were treated as nested spatial subsamples. Statistical analyses were conducted separately for each experimental site and aeration period. The two field sites were analyzed independently because they represented distinct experimental environments with different soil physicochemical properties. Treatment differences were evaluated using one-way analysis of variance (ANOVA), followed by Duncan's multiple range test at $p < 0.05$. Before parametric analyses, data normality and homogeneity of variance were evaluated. Values below the limit of quantification (LOQ) were treated as non-detectable (ND) and were not included in quantitative statistical comparisons. All figures were prepared using OriginPro 9.1.

3. Results

3.1. Establishment of the MITC Extraction Method from Activated Carbon

The specific treatments and recovery results of the L9 (3^3) orthogonal experiment are presented in Table 2. The recovery efficiencies of MITC obtained under the nine extraction conditions ranged from 69.1% to 103.5%, indicating that the extraction parameters affected the desorption efficiency of MITC from activated carbon.

Table 2. Orthogonal experimental design and MITC recovery results.

Experiment Number	Factor			REC (%)
	A	B	C	
1	1	1	1	89.8
2	1	2	3	103.5
3	1	3	2	99.1
4	2	1	3	71.5
5	2	2	2	73.4
6	2	3	1	69.1
7	3	1	2	87.4
8	3	2	1	84.2
9	3	3	3	94.8
K1	97.5	82.9	81	
K2	71.3	87	86.6	
K3	88.8	87.7	89.9	
R	26.1	4.8	8.9	

K1, K2, and K3 represent the mean MITC recoveries obtained at levels 1, 2, and 3 of each factor, respectively; R represents the difference between the maximum and minimum K values.

Range analysis was conducted to evaluate the relative contribution of each factor to MITC recovery. The results showed that the influence order of the investigated factors was extraction method (A) > activated carbon-to-solvent ratio (C) > extraction time (B), with range values of 26.1, 8.9, and 4.8, respectively. Among the three factors, extraction method exhibited the largest variation in recovery efficiency, suggesting that the interaction between extraction solvent and activated carbon was the dominant factor controlling MITC desorption. For extraction method (factor A), oscillatory extraction showed higher recovery efficiency than the other extraction approaches, which was likely due to enhanced contact between ethyl acetate and activated carbon during continuous agitation. For extraction time (factor B), recovery increased slightly with prolonged extraction, indicating that sufficient solvent–carbon interaction favored MITC release. For factor C, increasing the solvent proportion improved MITC recovery, possibly because a higher solvent volume increased the dissolution capacity of MITC and reduced the possibility of re-adsorption onto activated carbon. According to the range analysis, the theoretical optimal combination was A1B3C3. However, considering both extraction efficiency and solvent consumption, the condition of A1B3C2 was selected for subsequent experiments, corresponding to ethyl acetate extraction with an activated-carbon-to-solvent mass ratio of 1:1 and an extraction time of 120 min.

The ANOVA results are summarized in Table 3. The results were consistent with the range analysis, showing that extraction method and activated-carbon-to-solvent ratio contributed more strongly to recovery variation than extraction time.

Table 3. ANOVA decomposition of the unreplicated L9 orthogonal screening experiment.

Source	Sum of Squares	Degrees of Freedom	Mean Square	F	*p*-Value
A	1063.147	2	531.573	231.791	0.0043
B	40.207	2	20.103	8.766	0.1024
C	121.46	2	60.73	26.481	0.0364
Residual	4.587	2	2.293	—	—
Total	1229.4	8	—	—	—

Because each L9 combination was performed once, the residual term represents unexplained variation rather than independently estimated pure experimental error. Therefore, the F tests are presented as exploratory measures of relative factor importance.

The optimized extraction procedure was further validated to evaluate the analytical performance of MITC determination in activated carbon. To evaluate the quantitative linearity of MITC determination in ethyl acetate extracts, a solvent-based calibration curve was established over the concentration range of 0.005–10 mg L^{-1}, independently of the headspace calibration described in Section 2.6. The calibration curve was fitted using 1/x-weighted linear regression, with a coefficient of determination (R^2) of 0.9996. Examination of calibration residuals showed no obvious concentration-dependent deviation, indicating satisfactory linear response within the tested range.

The LOQ of MITC in activated carbon was determined based on recovery and precision experiments. Four fortification levels (0.01, 0.1, 1, and 5 mg kg^{-1}) were evaluated, with five independently prepared replicates at each level. Following the analytical performance criteria described in SANTE/11312/2021, the lowest validated fortification level meeting the acceptable recovery and precision requirements was considered as the LOQ. Since the recovery and precision results at 0.01 mg kg^{-1} met the acceptance criteria, the validated LOQ for MITC determination in activated carbon was established as 0.01 mg kg^{-1}.

The recovery results are summarized in Table 4. The mean recoveries of MITC from activated carbon ranged from 84.5% to 98.6%, with relative standard deviations (RSDs) of 1.8–8.0%, demonstrating satisfactory extraction accuracy and precision across the validated concentration range. The suitability of the established extraction procedure was supported by previously reported MITC analytical methods based on charcoal sorbents and ethyl-acetate-based desorption procedures. The validated extraction method was subsequently applied for the determination of MITC captured by the activated-carbon-coupled SVE system.

Table 4. MITC recoveries and relative standard deviations at four spiking levels.

Added Dose (mg kg^{-1})	Day 1		Day 2		Day 3		RSDB
	REC (%)	RSDN	REC (%)	RSDN	REC (%)	RSDN	
0.01	86.4	2.6	84.5	2.7	85.2	4.1	6.8
0.1	89.6	3.5	87.1	3.1	85.8	3.1	7.2
1	92.4	1.8	89.4	4.6	87.6	5.6	8.0
5	98.6	3.4	95.4	2.8	92.4	3.5	5.8

3.2. Temporal Changes in MITC Concentrations During SVE Operation

Gas- and solid-phase MITC concentrations before and after SVE at the Shunyi and Fangshan sites are shown in Table 5. Gas-phase and soil-phase MITC concentrations measured before and after SVE operation at the Fangshan and Shunyi sites are presented in Table 5. At Shunyi, the mean gas-phase MITC concentration obtained from uniform sampling was 0.051 ± 0.016 μg mL^{-1} before SVE, whereas the corresponding concentrations after operation were below the limit of quantification (LOQ, 0.001 μg mL^{-1}). At Fangshan, gas-phase MITC concentrations were below the LOQ at both sampling times. Therefore, exact percentage reductions in gas-phase MITC concentrations were not calculated. In contrast, soil-phase MITC concentrations increased between the two sampling times at both sites.

Soil-phase MITC concentrations increased between the pre- and post-SVE sampling times at both sites. However, this observation alone does not establish the underlying mechanism, as the changes may reflect continued DZ transformation, redistribution of MITC among soil phases, spatial heterogeneity, or differences between sampling locations.

The post-/pre-SVE concentration ratio declined as distance from the extraction pipe increased: from approximately 19-fold to 15-fold between 0.5 and 1.5 m in Fangshan and from approximately 9-fold to 6-fold over the same distance in Shunyi.

Table 5. Gas-phase and soil-phase MITC concentrations before and after SVE operation at the Fangshan and Shunyi field sites.

Site	Sampling Position (cm)	Gas Before SVE (μg mL^{-1})	Gas After SVE (μg mL^{-1})	Soil Before SVE (μg g^{-1})	Soil After SVE (μg g^{-1})	Soil-Phase MITC, Paired *p* Value
Fangshan	Uniform sampling	<LOQ	<LOQ	0.156 ± 0.032	2.766 ± 0.518	0.0126
	−50	<LOQ	<LOQ	0.172 ± 0.026	2.050 ± 0.642	0.0364
	0	<LOQ	<LOQ	0.143 ± 0.017	3.542 ± 0.268	0.0020
	50	<LOQ	<LOQ	0.160 ± 0.020	3.214 ± 0.426	0.0063
	100	<LOQ	<LOQ	0.155 ± 0.061	2.754 ± 0.189	0.0017
	150	<LOQ	<LOQ	0.162 ± 0.066	2.515 ± 0.361	0.0074
Shunyi	Uniform sampling	0.051 ± 0.016	<LOQ	0.325 ± 0.042	2.425 ± 0.434	0.0136
	−50	0.047 ± 0.003	<LOQ	0.348 ± 0.060	2.230 ± 0.550	0.0266
	0	0.034 ± 0.011	<LOQ	0.367 ± 0.041	3.053 ± 0.554	0.0137
	50	0.052 ± 0.008	<LOQ	0.294 ± 0.024	2.850 ± 0.443	0.0097
	100	0.015 ± 0.005	<LOQ	0.311 ± 0.032	2.315 ± 0.254	0.0052
	150	0.062 ± 0.021	<LOQ	0.281 ± 0.042	2.103 ± 0.330	0.0107

Values are presented as mean ± SD (n = 3 independent field plots). Before- and after-SVE soil-phase MITC concentrations were compared using paired-samples t-tests at the plot level. Gas-phase MITC concentrations below the LOQ were excluded from quantitative statistical comparisons.

3.3. MITC Adsorption by Activated Carbon During SVE Operation

The amounts of MITC recovered from the activated-carbon tubes and their corresponding average recovery rates during SVE operation are presented in Figure 2. Greater MITC recovery was observed at Fangshan than at Shunyi. At Fangshan, the average MITC recovery rate increased from 4.80 μg min^{-1} during the first 40 min to 9.7 μg min^{-1} during 120–160 min. In contrast, the corresponding rate at Shunyi decreased from 1.6 to 0.5 μg min^{-1} over the same intervals. These results demonstrate that MITC was retained by the activated-carbon tubes during SVE operation and reveal differences in MITC recovery patterns between the two field sites.

3.4. Effect of SVE on Cucumber Seedling Growth

Cucumber responses at 0 and 7 days of aeration are summarized in Table 6. At 0 days, fumigated soils from both sites caused marked phytotoxicity, with low germination before and immediately after SVE. After 7 days, however, SVE-treated soils from both sites supported 100% germination, comparable to their controls. In Fangshan, soil sampled before SVE still reduced germination and seedling growth after 7 days, whereas the corresponding SVE-treated soil showed no reduction and produced longer roots than the control. In Shunyi, SVE-treated soil also produced longer roots than the control. These results indicate that soils collected after SVE exhibited lower residual phytotoxicity than the corresponding fumigated no-SVE control soils following 7 days of laboratory aeration, as reflected by higher cucumber germination rates and favorable seedling growth under the tested bioassay conditions.

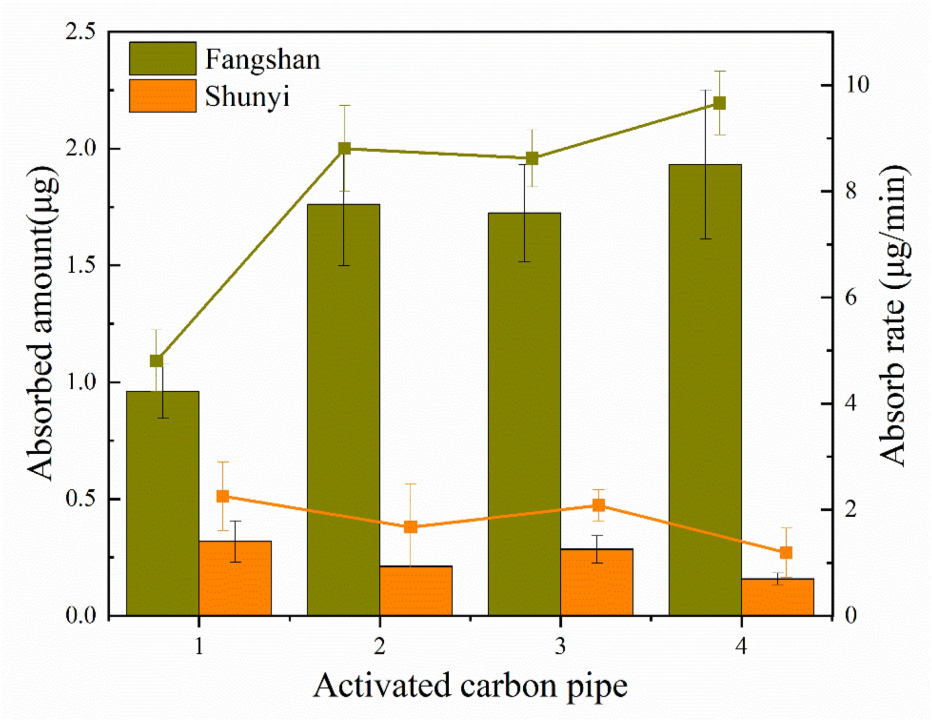

Figure 2. Cumulative amounts of MITC recovered from activated-carbon tubes and average MITC recovery rates during SVE operation at the Shunyi and Fangshan sites.

Table 6. Cucumber growth responses in soils subjected to SVE or natural aeration after dazomet fumigation.

Aeration Time (d)	Trial Site		Germination Rate (%)	Root Length (cm)	Shoot Length (cm)
0	Fangshan	Before SVE	7 ± 6 b	–	–
		After SVE	0 c	–	–
		Fumigated no-SVE control	9 ± 5 b	–	–
		Unfumigated control	100 ± 0 a	6.5 ± 0.6	8.4 ± 0.9
	Shunyi	Before SVE	0 c	–	–
		After SVE	17 ± 6 b	–	–
		Fumigated no-SVE control	0 c	–	–
		Unfumigated control	97 ± 6 a	6.8 ± 0.3	8.2 ± 0.7
7	Fangshan	Before SVE	70 ± 10 b	6.5 ± 0.8 b	7.2 ± 0.6 b
		After SVE	100 ± 0 a	8.6 ± 0.5 a	9.9 ± 0.4 a
		Fumigated no-SVE control	66 ± 8 b	6.3 ± 1.1 b	7.4 ± 0.9 b
		Unfumigated control	97 ± 6 a	7.2 ± 0.6 b	8.9 ± 0.6 a
	Shunyi	Before SVE	90 ± 0 a	8.1 ± 0.8 ab	9.4 ± 1.1 a
		After SVE	100 ± 0 a	8.5 ± 0.6 a	10.2 ± 0.7 a
		Fumigated no-SVE control	74 ± 6 b	7.8 ± 1.3 ab	9.0 ± 1.4 a
		Unfumigated control	100 ± 0 a	6.9 ± 0.7 b	8.9 ± 1.1 a

Before SVE, soil collected from the designated SVE plots immediately before initiation of SVE; after SVE, soil collected from the same plots immediately after completion of SVE; fumigated no-SVE control, soil collected at the corresponding time from concurrently DZ-fumigated plots that did not undergo SVE; unfumigated control, soil without DZ treatment used as a baseline reference for normal cucumber growth. "–" indicates that seedlings had not germinated or were too small to permit reliable measurement of root or shoot length. For each site, soil source, and aeration time, three independent field plots were used as experimental replicates (n = 3). Within each plot, 12 spatially distributed soil samples were collected and tested separately in 12 pots, with 10 seeds per pot; these pots were treated as within-plot spatial subsamples rather than independent field replicates. Values are presented as the mean ± SD of the three plot-level means. Within each site and aeration time, different lowercase letters indicate significant differences among soil treatments according to Duncan's multiple range test ($p \leq 0.05$).

4. Discussion

4.1. Temporal Changes and Potential Redistribution of MITC During SVE Operation

The increase in soil-phase MITC concentrations observed during SVE operation may reflect several concurrent processes. Continued transformation of residual DZ to MITC could contribute to the observed increase, while redistribution of MITC among soil phases and spatial variability in soil sampling may also influence the measured concentrations. In principle, SVE-induced changes in soil gas movement and concentration gradients could affect MITC redistribution and potentially influence DZ transformation. However, this remains an unconfirmed hypothesis, as residual DZ concentrations were not measured and a DZ–MITC mass balance was not established. This interpretation is also consistent with the mass-transfer principles widely documented for soil vapor extraction of volatile organic compounds [23–25]. Previous studies have also shown that SVE efficiency decreases with increasing distance from the extraction point [26,27].

Soil moisture may have been an important factor influencing SVE performance. The higher initial moisture content in Shunyi likely reduced air-filled porosity and restricted gas-flow pathways, thereby weakening the mass-transfer driving force and potentially limiting the enhancement of DZ conversion. This interpretation is consistent with previous studies showing that increasing soil moisture can reduce gas permeability and SVE efficiency [19,28,29]. However, because only two field sites were evaluated, differences in other soil physicochemical properties may also have contributed to the contrasting responses observed between Fangshan and Shunyi. Therefore, the role of soil moisture should be regarded as a plausible contributing factor rather than as a uniquely established cause. The declining enhancement with increasing distance from the extraction pipe is also consistent with radial attenuation of the vacuum driving force, a characteristic feature of SVE systems [18,30,31].

4.2. MITC Adsorption by Activated Carbon and Implications for Emission Management

Uncontrolled fumigant emission during film removal is a well-recognized environmental risk, with potential adverse effects on non-target organisms and ambient air quality [14,32]. The activated carbon adsorption unit integrated into the SVE system addresses this issue by capturing volatilized MITC before atmospheric release [33–35].

The divergent temporal adsorption trends between the two sites may be partly associated with differences in soil moisture and the resulting gas permeability. In the relatively drier Fangshan soil, continuous extraction may have facilitated the establishment of more effective gas-flow pathways, thereby increasing MITC mass transfer toward the extraction pipe over time. In contrast, the higher soil moisture in Shunyi may have restricted air-filled pore space and gas transport, potentially contributing to the lower or declining extraction efficiency. Such moisture-related limitations have been reported previously in SVE applications [18,19,36]. Nevertheless, because other physicochemical differences between the two soils were not independently controlled, the observed site-specific patterns cannot be attributed to soil moisture alone. Further controlled experiments would be required to determine the relative contribution of moisture and other soil properties. Although activated-carbon adsorption may provide a potential means of retaining MITC extracted from soil, its effectiveness in mitigating atmospheric emissions requires further verification through direct inlet–outlet concentration measurements, breakthrough assessments, and comparative field emission measurements.

4.3. Implications for Phytotoxicity Management and Sustainable Fumigation

Previous studies on compounds such as dimethyl disulfide (DMDS) and chloropicrin (CP) have shown that soil residues after membrane removal vary depending on application

rate, temperature, soil moisture, and soil texture, indicating that appropriate aeration durations may differ among regions and soil types [22,37,38]. For example, previous work reported that DMDS applied at 50 g m^{-2} in black soil required 21 days of aeration to ensure crop safety, whereas 14 days were still required in sandy loam, where dissipation was faster. Extended aeration periods reduce cropping-system efficiency, with natural aeration often requiring 14–21 days depending on soil properties and fumigant dosage [22]. In the present study, soils collected after SVE supported 100% cucumber germination following 7 days of laboratory aeration, whereas germination rates in the corresponding fumigated no-SVE control soils remained at 66–74%. These findings suggest that SVE treatment was associated with reduced residual phytotoxicity under the tested laboratory conditions. However, because the bioassay was conducted using field-collected soils maintained in open containers under laboratory conditions, rather than through direct crop establishment in the field, the results cannot establish whether SVE shortens the post-fumigation interval required for safe planting under field conditions. Further field validation is therefore necessary to determine the practical implications of this approach for crop establishment. Enhanced gas-phase mass transfer during and after SVE may also have contributed to faster dissipation of bioavailable MITC.

Notably, greater cucumber root length was observed in fumigated soils following SVE treatment. Previous studies have reported that soil fumigation can temporarily alter nutrient availability, nitrogen mineralization, and microbial activity, which may in some cases promote subsequent plant growth [39–41].

4.4. Limitations and Future Perspectives

Several limitations should be considered when interpreting the present results. First, although three independent SVE-treated plots and three concurrently fumigated no-SVE control plots were established at each field site, gas-phase and soil-phase MITC concentrations were measured only in the SVE-treated plots. The before-and-after sampling design allowed temporal changes in MITC concentrations to be characterized within the same field plots, thereby reducing potential variability associated with comparisons between different plots. However, the absence of corresponding MITC measurements from the no-SVE control plots prevented the effects of active vapor extraction from being distinguished from natural temporal changes, including continued DZ transformation, MITC volatilization, and phase redistribution. Therefore, the observed changes in MITC concentrations cannot be attributed exclusively to SVE. Second, residual DZ was not directly quantified, and a complete DZ–MITC mass balance was not established, limiting mechanistic interpretation. Furthermore, soil gas transport parameters, including air permeability, were not directly measured. Future studies should incorporate concurrent MITC measurements in SVE-treated and no-SVE control plots, direct quantification of residual DZ, and characterization of soil gas transport properties to better determine the contribution of SVE to MITC dissipation and redistribution under field conditions. In addition, although MITC was recovered from the activated-carbon tubes, neither adsorption breakthrough nor MITC concentrations downstream of the adsorption unit were determined. Direct measurements of atmospheric emission fluxes were also unavailable. Consequently, the MITC capture efficiency and potential emission reduction performance of the system remain to be established.

5. Conclusions

This study evaluated an activated-carbon-coupled soil vapor extraction (SVE) system for post-fumigation management of methyl isothiocyanate (MITC) following dazomet application. The optimized ethyl acetate extraction procedure provided satisfactory ana-

lytical recoveries of 84.5–98.6%. During field SVE operation, MITC was recovered from activated-carbon cartridges, demonstrating retention of a portion of the extracted fumigant. Changes in gas-phase and soil-phase MITC concentrations were also observed within the SVE-treated plots. However, because concurrent MITC measurements from fumigated no-SVE control plots were unavailable, these temporal changes could not be attributed exclusively to SVE.

Following 7 days of laboratory aeration, soils collected from the SVE-treated plots supported 100% cucumber germination at both field sites, compared with 66–74% in the corresponding fumigated no-SVE control soils. These results indicate lower residual phytotoxicity associated with SVE treatment under the tested laboratory bioassay conditions. Nevertheless, the present study did not establish whether SVE accelerated dazomet transformation, reduced atmospheric MITC emissions, or shortened the safe planting interval under field conditions. Further studies incorporating concurrent MITC controls, direct emission measurements, and field crop establishment trials are needed to evaluate the practical environmental and agronomic benefits of this approach.

Author Contributions: Conceptualization and methodology, Y.Z., X.T., Y.J., Y.L., W.F., D.Y., A.C. and Q.W.; formal analysis, Y.Z., X.T., Y.J., Y.L., W.F. and A.C.; investigation, Y.Z. and X.T.; resources, Y.L., D.Y. and Q.W.; writing—original draft preparation, Y.Z.; writing—review and editing, Y.J. and Q.W.; supervision, D.Y. and Q.W.; project administration, Q.W.; funding acquisition, Y.Z. and Q.W. All authors have read and agreed to the published version of the manuscript.

Funding: This research was funded by the Ministry of Science and Technology of the People's Republic of China through the National Key Research and Development Program of China (grant number 2023YFD1701200), and by the National Natural Science Foundation of China (grant number 32502561).

Institutional Review Board Statement: Not applicable. This study did not involve humans or animals.

Informed Consent Statement: Not applicable.

Data Availability Statement: The data presented in this study are available on request from the corresponding author. The data are not publicly available due to unstandardized site-specific notes and internal management information contained in the raw field-trial observation records.

Conflicts of Interest: The authors declare no conflicts of interest. The funders had no role in the design of the study; in the collection, analyses, or interpretation of data; in the writing of the manuscript; or in the decision to publish the results.

Abbreviations

The following abbreviations are used in this manuscript:

ANOVA	Analysis of variance
CK	Untreated control
DMDS	Dimethyl disulfide
DZ	Dazomet
GC–MS	Gas chromatography–mass spectrometry
LOQ	Limit of quantification
MITC	Methyl isothiocyanate
PE	Polyethylene
REC	Recovery
RSDB	Between-day relative standard deviation
RSDN	Within-day relative standard deviation
SIM	Selected ion monitoring
SVE	Soil vapor extraction
VOC	Volatile organic compound

References

1. Hou, D.; Jia, X.; Wang, L.; McGrath, S.P.; Zhu, Y.-G.; Hu, Q.; Zhao, F.-J.; Bank, M.S.; O'Connor, D.; Nriagu, J. Global soil pollution by toxic metals threatens agriculture and human health. *Science* **2025**, *388*, 316–321. [CrossRef] [PubMed]
2. Cao, A.C.; Liu, X.M.; Guo, M.X.; Wang, Q.X.; Li, Y.; Ouyang, C.B.; Yan, D.D. Incidences of soil-borne diseases and control measures. *Plant Prot.* **2017**, *43*, 6–16. [CrossRef]
3. Ślusarski, C.; Pietr, S.J. Combined application of dazomet and *Trichoderma asperellum* as an efficient alternative to methyl bromide in controlling the soil-borne disease complex of bell pepper. *Crop Prot.* **2009**, *28*, 668–674. [CrossRef]
4. Lin, C.-M.; Preston, J.F., III; Wei, C.-I. Antibacterial mechanism of allyl isothiocyanate. *J. Food Prot.* **2000**, *63*, 727–734. [CrossRef] [PubMed]
5. Littke, M.H.; LePage, J.; Sullivan, D.A.; Hebert, V.R. Comparison of field methyl isothiocyanate flux following Pacific Northwest surface-applied and ground-incorporated fumigation practices. *Pest Manag. Sci.* **2013**, *69*, 620–626. [CrossRef] [PubMed]
6. Fritsch, H.J.; Huber, R. Basamid granular—A halogen-free soil disinfestant. *Acta Hortic.* **1995**, *382*, 76–85. [CrossRef]
7. Swancutt, K.L.; Dail, M.K.; Mezyk, S.P.; Ishida, K.P. Absolute kinetics and reaction efficiencies of hydroxyl-radical-induced degradation of methyl isothiocyanate (MITC) in different quality waters. *Chemosphere* **2010**, *81*, 339–344. [CrossRef] [PubMed]
8. Matthiessen, J.N.; Shackleton, M.A. Biofumigation: Environmental impacts on the biological activity of diverse pure and plant-derived isothiocyanates. *Pest Manag. Sci.* **2005**, *61*, 1043–1051. [CrossRef] [PubMed]
9. Zheng, W.; Yates, S.R.; Papiernik, S.K.; Guo, M. Effect of combined application of methyl isothiocyanate and chloropicrin on their transformation. *J. Environ. Qual.* **2004**, *33*, 2157–2164. [CrossRef] [PubMed]
10. Zhang, Y.; Fang, W.; Yan, D.; Ji, Y.; Chen, X.; Guo, A.; Song, Z.; Li, Y.; Cao, A.; Wang, Q. Comparison of drip-irrigated or injected allyl isothiocyanate against key soil-borne pathogens and weeds. *Pest Manag. Sci.* **2023**, *79*, 3860–3870. [CrossRef] [PubMed]
11. Frick, A.; Zebarth, B.J.; Szeto, S.Y. Behavior of the soil fumigant methyl isothiocyanate in repacked soil columns. *J. Environ. Qual.* **1998**, *27*, 1158–1169. [CrossRef]
12. Simpson, C.R.; Nelson, S.D.; Stratmann, J.E.; Ajwa, H.A. Surface water seal application to minimize volatilization loss of methyl isothiocyanate from soil columns. *Pest Manag. Sci.* **2010**, *66*, 686–692. [CrossRef] [PubMed]
13. Castellano-Hinojosa, A.; Boyd, N.S.; Strauss, S.L. Impact of fumigants on non-target soil microorganisms: A review. *J. Hazard. Mater.* **2022**, *427*, 128149. [CrossRef] [PubMed]
14. Kyung, Y.; Kim, H.K.; Lee, J.S.; Kim, B.-S.; Yang, J.-O.; Lee, B.-H.; Koo, H.-N.; Kim, G.-H. Efficacy and phytotoxicity of phosphine as fumigants for *Frankliniella occidentalis* (Thysanoptera: Thripidae) on asparagus. *J. Econ. Entomol.* **2018**, *111*, 2644–2651. [CrossRef] [PubMed]
15. Fang, W.; Yan, D.; Wang, X.; Huang, B.; Wang, X.; Liu, J.; Liu, X.; Li, Y.; Ouyang, C.; Wang, Q.; et al. Responses of nitrogen-cycling microorganisms to dazomet fumigation. *Front. Microbiol.* **2018**, *9*, 2529. [CrossRef] [PubMed]
16. Stewart, L.; Lutes, C.; Truesdale, R.; Schumacher, B.; Zimmerman, J.H.; Connell, R. Field study of soil vapor extraction for reducing off-site vapor intrusion. *Groundw. Monit. Remediat.* **2020**, *40*, 74–85. [CrossRef] [PubMed]
17. Johnson, P.C.; Ettinger, R.A. Heuristic model for predicting the intrusion rate of contaminant vapors into buildings. *Environ. Sci. Technol.* **1991**, *25*, 1445–1452. [CrossRef]
18. Liu, Y.; Huang, F.; Zhou, D.; Wang, T.; Wang, G. Study of factors affecting the remediation of contaminated soil through pneumatic fracturing and soil vapor extraction. *J. Hazard. Mater.* **2024**, *467*, 133776. [CrossRef] [PubMed]
19. Lopez-Canfin, C.; Lázaro, R.; Sánchez-Cañete, E.P. Water vapor adsorption by dry soils: A potential link between the water and carbon cycles. *Sci. Total Environ.* **2022**, *824*, 153746. Correction in *Sci. Total Environ.* **2023**, *874*, 162457. https://doi.org/10.1016/j.scitotenv.2023.162457. [CrossRef] [PubMed]
20. Zhang, P.; Zhao, F.; Shi, W.; Lu, H.; Zhou, X.; Guo, Y.; Yu, G. Super water-extracting gels for solar-powered volatile organic compounds management in the hydrological cycle. *Adv. Mater.* **2022**, *34*, 2110548. [CrossRef] [PubMed]
21. Kuppusamy, S.; Palanisami, T.; Megharaj, M.; Venkateswarlu, K.; Naidu, R. In-situ remediation approaches for the management of contaminated sites: A comprehensive overview. In *Reviews of Environmental Contamination and Toxicology*; de Voogt, P., Ed.; Springer International Publishing: Cham, Switzerland, 2016; Volume 236, pp. 1–115. [CrossRef] [PubMed]
22. Wang, X.; Zhang, Y.; Cao, A.; Xu, J.; Fang, W.; Yan, D.; Li, Y.; Wang, Q. Effects of soil type, moisture content and organic amendment rate on dimethyl disulfide distribution and persistency in soil. *Environ. Pollut.* **2021**, *285*, 117198. [CrossRef] [PubMed]
23. Cao, W.; Zhang, L.; Miao, Y.; Qiu, L. Research progress in the enhancement technology of soil vapor extraction of volatile petroleum hydrocarbon pollutants. *Environ. Sci. Process. Impacts* **2021**, *23*, 1650–1662. [CrossRef] [PubMed]
24. Rathfelder, K.; Lang, J.R.; Abriola, L.M. Soil vapor extraction and bioventing: Applications, limitations, and future research directions. *Rev. Geophys.* **1995**, *33*, 1067–1081. [CrossRef]
25. Schulenberg, J.W.; Reeves, H.W. Axi-symmetric simulation of soil vapor extraction influenced by soil fracturing. *J. Contam. Hydrol.* **2002**, *57*, 189–222. [CrossRef] [PubMed]

26. Xue, Y.; Liu, J.; Liang, X.; Wang, S.; Ma, Z. Ecological risk assessment of soil and water loss by thermal enhanced methane recovery: Numerical study using two-phase flow simulation. *J. Clean. Prod.* **2022**, *334*, 130183. [CrossRef]
27. Xue, Y.; Liu, J.; Ranjith, P.G.; Liang, X.; Wang, S. Investigation of the influence of gas fracturing on fracturing characteristics of coal mass and gas extraction efficiency based on a multi-physical field model. *J. Pet. Sci. Eng.* **2021**, *206*, 109018. [CrossRef]
28. Yoon, H.; Valocchi, A.J.; Werth, C.J. Modeling the influence of water content on soil vapor extraction. *Vadose Zone J.* **2003**, *2*, 368–381. [CrossRef]
29. Simpanen, S.; Yu, D.; Mäkelä, R.; Talvenmäki, H.; Sinkkonen, A.; Silvennoinen, H.; Romantschuk, M. Soil vapor extraction of wet gasoline-contaminated soil made possible by electroosmotic dewatering–lab simulations applied at a field site. *J. Soils Sediments* **2018**, *18*, 3303–3309. [CrossRef]
30. Nobre, M.M.M.; Nobre, R.C.M. Soil vapor extraction of chlorinated solvents at an industrial site in Brazil. *J. Hazard. Mater.* **2004**, *110*, 119–127. [CrossRef] [PubMed]
31. Halmemies, S.; Gröndahl, S.; Arffman, M.; Nenonen, K.; Tuhkanen, T. Vacuum extraction based response equipment for recovery of fresh fuel spills from soil. *J. Hazard. Mater.* **2003**, *97*, 127–143. [CrossRef] [PubMed]
32. Castellano-Hinojosa, A.; Karlsen-Ayala, E.; Boyd, N.S.; Strauss, S.L. Impact of repeated fumigant applications on soil properties, crop yield, and microbial communities in a plastic-mulched tomato production system. *Sci. Total Environ.* **2024**, *919*, 170659. [CrossRef] [PubMed]
33. Gan, J.; Megonnell, N.E.; Yates, S.R. Adsorption and catalytic decomposition of methyl bromide and methyl iodide on activated carbons. *Atmos. Environ.* **2001**, *35*, 941–947. [CrossRef]
34. Wood, J.P.; Clayton, M.J.; McArthur, T.; Serre, S.D.; Mickelsen, L.; Touati, A. Capture of methyl bromide emissions with activated carbon following the fumigation of a small building contaminated with a *Bacillus anthracis* spore simulant. *J. Air Waste Manag. Assoc.* **2015**, *65*, 145–153. [CrossRef] [PubMed]
35. Yang, Y.; Li, Y.; Walse, S.S.; Mitch, W.A. Destruction of methyl bromide sorbed to activated carbon by thiosulfate or electrolysis. *Environ. Sci. Technol.* **2015**, *49*, 4515–4521. [CrossRef] [PubMed]
36. Farhan, S.; Holsen, T.M.; Budiman, J. Interaction of soil air permeability and soil vapor extraction. *J. Environ. Eng.* **2001**, *127*, 32–37. [CrossRef]
37. Stevens, M.; Freeman, J. Soil persistence of dimethyl disulfide combined with chloropicrin after repeated applications. *Crop Prot.* **2017**, *98*, 143–148. [CrossRef]
38. Tang, X.; Cao, A.; Zhang, Y.; Chen, X.; Hao, B.; Xu, J.; Fang, W.; Yan, D.; Li, Y.; Wang, Q. Soil properties affect vapor-phase adsorption to regulate dimethyl disulfide diffusion in soil. *Sci. Total Environ.* **2022**, *825*, 154012. [CrossRef] [PubMed]
39. Fang, W.; Huang, B.; Sun, Y.; Yan, D.; Li, Y.; Tilocca, B.; Roncada, P.; Wang, Q.; Cao, A. Soil amendments promoting nitrifying bacteria recovery faster than the denitrifying bacteria at post soil fumigation. *Sci. Total Environ.* **2024**, *908*, 168041. [CrossRef] [PubMed]
40. Eo, J.; Park, K.-C. Effects of dazomet on soil organisms and recolonisation of fumigated soil. *Pedobiologia* **2014**, *57*, 147–154. [CrossRef]
41. Chen, R.; Jiang, W.; Xu, S.; Fan, H.; Chen, X.; Shen, X.; Yin, C.; Mao, Z. An emerging chemical fumigant: Two-sided effects of dazomet on soil microbial environment and plant response. *Environ. Sci. Pollut. Res.* **2022**, *29*, 3022–3036. [CrossRef] [PubMed]

Disclaimer/Publisher's Note: The statements, opinions and data contained in all publications are solely those of the individual author(s) and contributor(s) and not of MDPI and/or the editor(s). MDPI and/or the editor(s) disclaim responsibility for any injury to people or property resulting from any ideas, methods, instructions or products referred to in the content.